

# Quantification of Fluoroquinolone Uptake through the Outer Membrane Channel OmpF of *Escherichia coli*

Jehangir Cama,<sup>†,‡</sup> Harsha Bajaj,<sup>‡,§</sup> Stefano Pagliara,<sup>†,§</sup> Theresa Maier,<sup>†</sup> Yvonne Braun,<sup>‡</sup> Mathias Winterhalter,<sup>‡</sup> and Ulrich F. Keyser<sup>\*,†</sup>

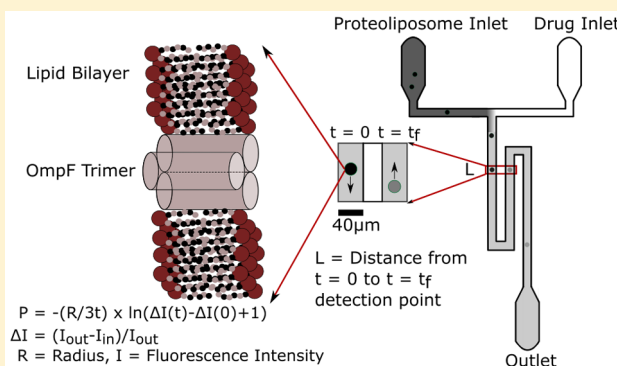
<sup>†</sup>Biological and Soft Systems, Cavendish Laboratory, Department of Physics, University of Cambridge, JJ Thomson Avenue, Cambridge CB3 0HE, United Kingdom

<sup>‡</sup>Jacobs University Bremen, Campus Ring 1, D-28759, Bremen, Germany

<sup>§</sup>Department of Biosciences, College of Life and Environmental Sciences, University of Exeter, Exeter, Devon EX4, United Kingdom

## S Supporting Information

**ABSTRACT:** Decreased drug accumulation is a common cause of antibiotic resistance in microorganisms. However, there are few reliable general techniques capable of quantifying drug uptake through bacterial membranes. We present a semi-quantitative optofluidic assay for studying the uptake of autofluorescent drug molecules in single liposomes. We studied the effect of the *Escherichia coli* outer membrane channel OmpF on the accumulation of the fluoroquinolone antibiotic, norfloxacin, in proteoliposomes. Measurements were performed at pH 5 and pH 7, corresponding to two different charge states of norfloxacin that bacteria are likely to encounter in the human gastrointestinal tract. At both pH values, the porins significantly enhance drug permeation across the proteoliposome membranes. At pH 5, where norfloxacin permeability across pure phospholipid membranes is low, the porins increase drug permeability by 50-fold on average. We estimate a flux of about 10 norfloxacin molecules per second per OmpF trimer in the presence of a 1 mM concentration gradient of norfloxacin. We also performed single channel electrophysiology measurements and found that the application of transmembrane voltages causes an electric field driven uptake in addition to concentration driven diffusion. We use our results to propose a physical mechanism for the pH mediated change in bacterial susceptibility to fluoroquinolone antibiotics.



## INTRODUCTION

Antimicrobial resistance is a daunting challenge, threatening to undermine the very fabric of modern medicine today.<sup>1–4</sup> The inexorable emergence of resistant organisms, coupled with a decline in the discovery of new antimicrobials, has led to a global public health crisis. The recent breakthrough discovery of a new antibiotic, teixobactin,<sup>5</sup> is extremely good news. However, its relative inactivity against Gram-negative pathogens shows that the battle against antimicrobial resistance will be extremely challenging.

Gram-negative bacteria have a hydrophobic double-membrane cell envelope that presents a barrier for hydrophilic molecules trying to enter the cell. The outer membrane (OM) is even more hydrophobic than a typical phospholipid membrane due to the presence of lipopolysaccharides (LPS), whose strong lateral interactions inhibit the passage of a variety of compounds through the OM.<sup>6</sup> Translocation across the OM is thus mainly governed by the presence of outer membrane protein “porins” that form water-filled channels allowing the diffusion of compounds through the OM.

Consequently, the down-regulation of these porins enables bacteria to escape the deleterious effects of antibiotics.<sup>6–9</sup> For example, a reduction in the expression of Outer membrane protein F (OmpF), a major porin found in *Escherichia coli*, has been associated with a decrease in the accumulation of fluoroquinolone antibiotics; this eventually gives rise to drug resistance.<sup>7,10–12</sup> Furthermore, antibiotic therapy results in a switch in porin expression from OmpF to the narrower OmpC; this is thought to be due to the high osmolarity conditions existing in patients under drug treatment.<sup>7</sup> This leads to a significant decrease in antibiotic accumulation within the cell, and hence a decrease in antibiotic susceptibility.<sup>7</sup> It is thus clear that understanding antibiotic accumulation in cells is crucial, and methods to better quantify antibiotic permeation are urgently required.<sup>13</sup>

Fluoroquinolones are broad-spectrum antibiotics that inhibit bacterial type II topoisomerases. These topoisomerases are

Received: June 11, 2015

Revised: August 24, 2015



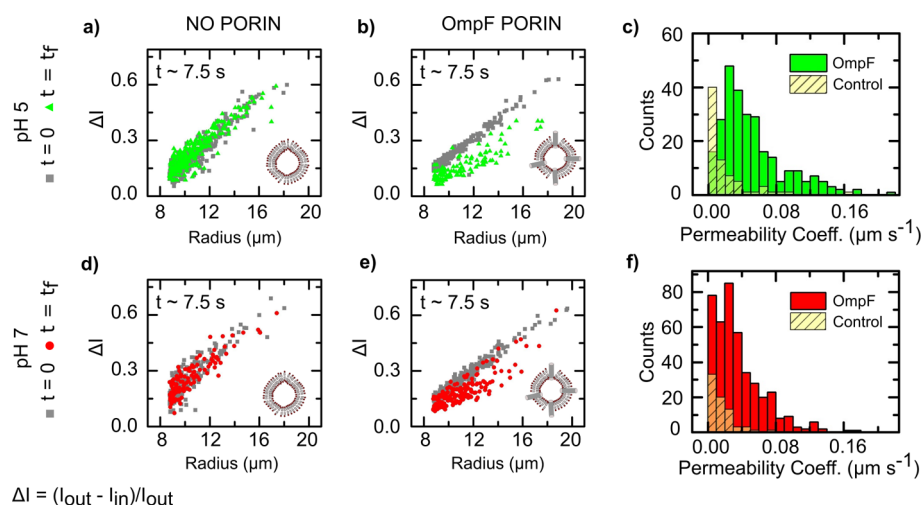


**Figure 1.** Optofluidic permeability assay (depicted schematically in Figure 3) shows the rapid uptake of norfloxacin in OmpF embedded proteoliposomes. Comparison of the uptake measurements in liposomes and proteoliposomes at pH 5 (a and b) and pH 7 (d and e). Each point references an uptake measurement at the single vesicle level, the gray points being  $t = 0$  and the green (pH 5) and red (pH 7) being the final detection point  $t = t_f$ . On average it took individual vesicles about 7.5 s to move from the initial to the final detection point. In the absence of porins (a,d), there is no shift in  $\Delta I$  values observed at the later time point at either pH. The presence of porins (b,e) leads to a marked downward shift in  $\Delta I$  for the majority of the proteoliposomes at the later detection point, both at pH 5 and pH 7. The downward shift in  $\Delta I$  corresponds to an increase in the norfloxacin autofluorescence intensity within the proteoliposome ( $I_{in}$ ), and is thus a direct measure of norfloxacin uptake. Scatter plots of other porin experiments are presented in the [Supporting Information](#). The histograms (c,f) are a record of permeability coefficients ( $P$ ) measured for individual porin-embedded proteoliposomes, and summarize the data from 3 separate experiments at each pH. Histograms from the control measurements with liposomes (no porins) are overlaid to show the shift in  $P$  due to the presence of porins in the membrane. Total liposomes/proteoliposomes detected were  $N = 268$  (pH 5, with porins),  $N = 74$  (pH 5, no porins),  $N = 420$  (pH 7, with porins) and  $N = 74$  (pH 7, no porins).

essential enzymes, involved in key cellular processes such as DNA replication.<sup>14</sup> Since their targets are intracellular, fluoroquinolones must pass through the outer and inner bacterial membrane to be effective.<sup>10</sup> The OM thus presents the initial diffusion barrier for drug uptake, and the accumulation of fluoroquinolone molecules in the periplasm ultimately determines their flux into the cytoplasm. Changes in bacterial susceptibility to fluoroquinolones due to changes in pH have been reported previously.<sup>15,16</sup> An increase in external pH from acidic to basic was shown to correspond to a reduction in the minimum inhibitory concentration (MIC) of norfloxacin.<sup>17</sup> Further, it was proposed that this pH mediated change in susceptibility is related to changes in the uptake of fluoroquinolones due to alterations of the electric charge of the antibiotic molecule;<sup>18,19</sup> norfloxacin, for example, is positively charged at pH 5 and neutral (zwitterionic, but a significant proportion are also uncharged) at pH 7.<sup>18,19</sup> It thus seems reasonable to assume that the fluoroquinolone susceptibility of bacteria in response to pH changes is a complicated process, which might involve both changes in porin expression<sup>20</sup> and changes in drug transport through porins in the OM as well as through the phospholipid inner membrane.

At acidic pH values, fluoroquinolone molecules carry charge<sup>18</sup> and thus transport across the OM should be strongly influenced by even relatively small potentials across the OM. Donnan potentials are known to exist across the OM due to the presence of anchored, anionic membrane-derived oligosaccharides (MDOs) in the *E. coli* periplasm.<sup>21,22</sup> The magnitude of these potentials depends strongly on the ionic concentration of the surrounding medium. At physiological ion concentrations, the Donnan potential is of the order of 20–30 mV, but variations of 5–100 mV have been reported by changing external cation concentrations.<sup>21</sup> One would expect such

changes to have a significant effect on the transport of charged molecules through OM porins.

For autofluorescent antibiotics like quinolones, the determination of antibiotic uptake via a cell ensemble recording has previously been suggested. However, the technique suffers from difficulties in distinguishing between antibiotic molecules that were accumulated inside versus those bound to the cell membrane.<sup>23</sup> More recently, fluorescence based single cell imaging enabled the comparison of feroxacin uptake in resistant versus susceptible bacteria.<sup>24</sup> However, barring these few exceptions, a quantitative analysis of fluoroquinolone transport through porins and lipids has proven technologically challenging.

In this study we describe an optofluidic assay that measures the permeability of antibiotics through porins exclusively in a proteoliposome system. OmpF porins are reconstituted into giant unilamellar vesicles and norfloxacin uptake into these proteoliposomes is tracked directly in a label-free manner using the UV autofluorescence of the drug. Patching the proteoliposomes reveals an estimate of the porin density, and combining the two measurements enables the calculation of norfloxacin translocation rates through OmpF channels in the proteoliposomes. Furthermore, proteoliposomes are cell-free systems, and thus active or passive uptake processes can be independently examined in highly controlled environments. We compare our measurements with single channel electrophysiology, and explore the combined effect of pH and transmembrane voltage on norfloxacin transport through OmpF.

## RESULTS

**Optofluidic Permeability Assay.** In the optofluidic permeability assay, OmpF embedded proteoliposomes (see [Methods](#)) are exposed to norfloxacin by controlled mixing in a

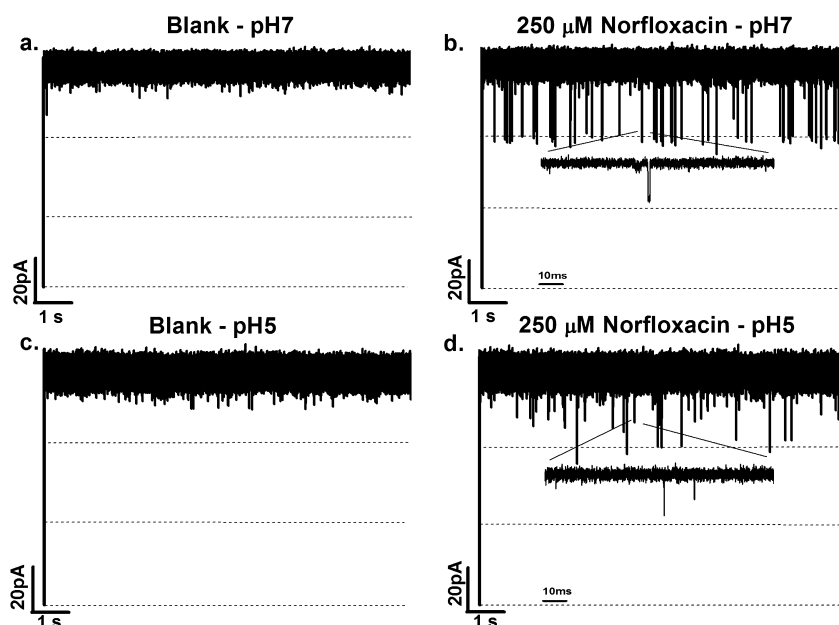


**Figure 2.** Ionic current traces of a single trimeric OmpF porin: (a) in the absence of antibiotics at pH 7, (b) with 250  $\mu\text{M}$  norfloxacin *cis* side at pH 7, (c) in the absence of antibiotics at pH 5 and (d) with 250  $\mu\text{M}$  norfloxacin *cis* side at pH 5. Electrolyte conditions: 1 M KCl, 5 mM acetate (pH 5) or 5 mM  $\text{PO}_4$  (pH 7). The applied voltage was  $-25$  mV. The dotted lines specify the ionic current levels through single monomers of the OmpF trimer. The addition of norfloxacin at pH 7 (b) leads to well resolved blockages of the ionic current through a monomer, whereas at pH 5 (d) the antibiotic molecules lead to flickering in the ionic current through a monomer; full blockages are not always observed. This is due to the low residence time of the antibiotic in the channel at pH 5, as discussed in the text.

T junction microfluidic chip. The vesicles (liposomes/proteoliposomes) are imaged under UV irradiation at two points, first immediately post mixing with the drug and then again after time  $t$ , a short distance further downstream. A comparison of the drug UV autofluorescence intensities within the vesicles at both points enables the direct visualization of drug uptake and the calculation of the permeability coefficient ( $P$ ) and flux ( $J$ ) of the drug through the vesicle membrane. This assay also allows the comparison of norfloxacin flux values through OmpF at different pH conditions in the absence of an applied transmembrane voltage.

The results of the optofluidic permeability assay are summarized in Figure 1; more results can be viewed in the Supporting Information Figure S1. The graphs (Figures 1a,b,d,e) show a normalized intensity difference ( $\Delta I = \{(I_{\text{out}} - I_{\text{in}})/I_{\text{out}}\}$ ) between the background autofluorescence intensity ( $I_{\text{out}}$ ) and the autofluorescence intensity inside the vesicle ( $I_{\text{in}}$ ), versus vesicle radius ( $R$ ). Each point represents a single vesicle measurement. The gray squares represent vesicles at the initial viewpoint immediately post mixing with the norfloxacin (which for convenience we set to  $t = 0$ ). The green triangles (pH 5) and red circles (pH 7) represent vesicles once they have traveled along the channel to the next detection position. The permeability coefficient ( $P$ ) is given by<sup>25</sup>

$$P = -\left(\frac{R}{3t}\right) \times \ln(\Delta I(t) - \Delta I(0) + 1)$$

where  $t$  is the time taken for the vesicle to move from the initial detection point to the final detection point (on average this was about 7.5 s). The norfloxacin concentration present in the channel after mixing is about 1 mM; at  $t = 0$ , there is no norfloxacin inside the vesicles, whereas outside the vesicles the concentration is 1 mM.

The experiments were performed at pH 5 and pH 7. In both cases the presence of OmpF causes a marked change in  $\Delta I$  indicating the rapid accumulation of the drug inside the proteoliposomes.

Control measurements in the absence of OmpF revealed a substantially slower uptake, indicating that OmpF porins significantly enhance the permeability of the membranes to norfloxacin. We can calculate the contributions to the flux from the porins and lipids separately; details are given in the Supporting Information. In the absence of porins, norfloxacin permeability is significantly higher at pH 7 than at pH 5.<sup>25</sup> In contrast, the presence of the porins leads to similar permeability coefficients at both pH 5 and pH 7. On average, the norfloxacin permeability increased approximately 50-fold (pH 5) and 6-fold (pH 7) due to the presence of OmpF in the membrane, leading to drug accumulation within the proteoliposomes in a matter of seconds rather than in minutes. The relative pH independence of the permeability in the presence of OmpF suggests that the charge of the molecule does not play a significant role in influencing its transport through the porin in the absence of a transmembrane potential.

The spread in the permeability coefficient histograms (Figure 1c,f) is caused by the inevitable variability of OmpF insertions into individual vesicles prepared for the optofluidics experiments. This can be seen in the scatter plots as well; it is clear that, at both pH conditions, a handful of vesicles do not show significant transport. It is known, however, that electroformation produces some multilamellar vesicles,<sup>26</sup> and in these the porins cannot insert across all membranes; this accounts for the few negative observations.

**Antibiotic Interaction with OmpF Using Single Channel Electrophysiology.** In this assay, electrophysiology was used to study the interaction of norfloxacin with OmpF channels reconstituted in planar lipid bilayers. Traditionally, a lipid bilayer is formed across an aperture in a Teflon film that

**Table 1. Antibiotic Association ( $k_{\text{on}}$ ) and Dissociation ( $k_{\text{off}}$ ) Rate Constants Obtained by Single Channel Measurements for OmpF at pH 5 and pH 7<sup>a</sup>**

$$k_{\text{on}} = (\{\text{No. of events/sec}\} / 3^*[\text{c}]), k_{\text{off}} = (1/\text{residence time})$$

$$J = \frac{k_{\text{on}}^{\text{cis}} \cdot c_{\text{cis}} \cdot k_{\text{on}}^{\text{trans}}}{(k_{\text{on}}^{\text{cis}} + k_{\text{on}}^{\text{trans}})}; \Delta c = 1 \text{ mM}; \text{ valid under } k_{\text{off}} \gg k_{\text{on}} \cdot c$$

antibiotics	$k_{\text{on}}^{\text{cis}} (10^3) \{1/(\text{s} \cdot \text{M})\}$	$k_{\text{on}}^{\text{trans}} (10^3) \{1/(\text{s} \cdot \text{M})\}$	$k_{\text{off}}^{\text{total}} 1/(\text{s})$	J (molecules/s)
Norfloxacin	−50 mV	+50 mV		$\Delta c = 1 \text{ mM}$
pH 7	$13 \pm 5$	1.3	$1561 \pm 120$	1
pH 5	$11 \pm 3$	10	25000	$5 \pm 1$
	−25 mV	+25 mV		
pH 7	$9 \pm 2.5$	1	$1150 \pm 60$	0.9
pH 5	$3 \pm 1$	$5 \pm 2$	27000	$1.8 \pm 0.7$
	0 mV (Optofluidics)			
pH 7				$10 \pm 8$
pH 5				$15 \pm 10$

<sup>a</sup>Electrolyte conditions: 1 M KCl, 5 mM PO<sub>4</sub> (pH 7)/acetate (pH 5). Errors are standard deviations.

separates two reservoirs in a cuvette. The reservoirs are filled with an electrolyte solution and a potential difference is applied across the lipid membrane via electrodes in the reservoirs. Porins are reconstituted in the lipid bilayer and their conductance properties studied by measuring the ionic current flowing through the membrane. The addition of antibiotics leads to blockages in the ionic current, since the antibiotic molecules displace ions flowing through the porin. A detailed description of the technique is provided in the [Methods](#) section.

We varied the transmembrane voltages (25 mV and 50 mV) to determine whether the charge on the norfloxacin molecule at pH 5 influenced its transport through the channel under an applied electric field comparable to the OM potentials in natural systems. In the absence of antibiotics, fluctuations in the ionic current through a single OmpF channel were negligible, both at pH 7 and pH 5 ([Figure 2a](#) and [2c](#)). The addition of 250  $\mu\text{M}$  norfloxacin to the extracellular (*cis*) side of the protein at pH 7 led to well resolved blockages of ionic current as shown in [Figure 2b](#).

At pH 5, the addition of 250  $\mu\text{M}$  norfloxacin gave rise to partial unresolved flickering in the ionic current ([Figure 2d](#)); the ionic current through a monomer was not completely blocked due to the presence of the antibiotic. This was due to the low residence times of the norfloxacin molecules in the channel at pH 5, as discussed below.

The kinetic rate constants (association and dissociation rates) characterizing the interaction of norfloxacin molecules with the OmpF channel were calculated as described previously;<sup>27</sup> these are quantified in [Table 1](#). Interestingly, the dissociation rate of the antibiotic varied by an order of magnitude at the different pH conditions. At pH 7 the residence time of the antibiotic in the channel was about 900  $\mu\text{s}$  (−25 mV experiments). However, at pH 5, when the molecule is positively charged, this is reduced to 40  $\mu\text{s}$  ([Table 1](#)). This imbalance in the pH 7 and pH 5 residence times was observed at the higher transmembrane voltage of −50 mV as well (650 and 40  $\mu\text{s}$  respectively).

The flux ( $J$  molecules/s) of norfloxacin through the channel was calculated based on a flux model valid for both symmetric and asymmetric transport through a channel.<sup>27–30</sup> When a transmembrane voltage of −25 mV was applied across the bilayer, the flux was found to be slightly higher at pH 5 (~2 molecules/s) than at pH 7 (~1 molecule/s). When the

transmembrane voltage was increased to −50 mV, the norfloxacin flux value at pH 5 increased to  $5 \pm 1$  molecules/s while the flux at pH 7 remained unchanged (1 molecule/s). An obvious explanation suggests that the positive charge on the norfloxacin molecules at pH 5 results in them being driven through the porin under an applied transmembrane voltage. At pH 7 the overall charge on the molecule is neutral and thus the effect of the transmembrane voltage on the flux seems less important; free diffusion appears to be the primary driving agent. However, there might still be some small voltage dependent effects since a significant proportion of the molecules are zwitterionic at pH 7—this requires further investigation.

Note that the flux was calculated using  $\Delta c = 1 \text{ mM}$ , to compare with the optofluidic permeability assay results described above. This is justified since it was observed that the number of antibiotic events in the ionic current recordings increased linearly with an increasing concentration of the antibiotic, and hence the rate constants measured with a concentration difference of 250  $\mu\text{M}$  were equally applicable at a concentration difference of 1 mM.

## DISCUSSION

In this study, we used a label-free optofluidic permeability assay alongside single channel electrophysiology to explore the pH and voltage dependence of norfloxacin transport through OmpF porins. The optofluidic assay directly proves that the uptake of norfloxacin is enhanced by OmpF reconstituted in the proteoliposomes.

An interesting pattern emerges: in the absence of any transmembrane potential, the optofluidics assay shows that the permeability of the proteoliposomes is essentially the same (within error) at both pH 5 and pH 7. However, as the transmembrane voltage is increased (in electrophysiology), the flux at pH 5 starts to increase over the flux at pH 7. At a transmembrane voltage close to typical physiological OM Donnan potentials<sup>21</sup> of −25 mV, the flux at pH 5 is twice as large as the flux at pH 7. On increasing the transmembrane voltage to −50 mV, the flux at pH 5 increases to five times that at pH 7. This confirms that the positive charge on norfloxacin at pH 5 contributes significantly to its transport across porins in the presence of transmembrane voltages.

It has been reported that a change in the pH from acidic to basic reduced the minimum inhibitory concentration (MIC) of



norfloxacin;<sup>17</sup> furthermore, the antibiotic showed maximum cytoplasmic accumulation at pH 7.5.<sup>18</sup> This agrees well with the data obtained in our study. As mentioned above, our experiments suggest that norfloxacin will likely accumulate in the periplasm (across the porin) of an *E. coli* bacterium at a 2× faster rate at pH 5 compared to pH 7. However, the drug molecules now encounter the phospholipid inner membrane (IM). Our previous work showed that the direct diffusion of norfloxacin through a pure vesicle lipid bilayer is more effective (by a factor of approximately 6×) at pH 7 than at pH 5.<sup>25</sup> Furthermore, the periplasmic pH is expected to be the same as the external pH.<sup>31</sup> Considering the relative rates of norfloxacin transport across the two membranes at pH 5 and pH 7 thus explains the higher cytoplasmic accumulation at neutral/slightly basic pH values.<sup>17,18</sup> This suggests that diffusion through the inner membrane might present the rate limiting step. However, it should also be noted that medium acidification leads to the preferential expression of the narrower OmpC porins over OmpF<sup>20</sup> in *E. coli*, which might further reduce norfloxacin accumulation at acidic pH values.

The optofluidics assay clearly proves that the presence of OmpF makes the resultant proteoliposomes more permeable to norfloxacin, with an increased flux of drug molecules through the proteoliposome membrane (the total flux through the membrane is given by  $J = P \times 4\pi R^2 \times \Delta c$ ). However, to estimate the flux *per porin* is not straightforward, since it is difficult to quantify the exact number of porins in each proteoliposome membrane.

To obtain a rough estimate of the flux per porin from the optofluidics assay, vesicles incubated with OmpF were patched and characterized electrically using a Port-a-Patch system (Nanion Technologies GmbH, Germany) (Supplementary Figure S2). Since the patched area is well-known (patch diameter = 1 μm) and the number of porin insertions counted (using the ionic current characteristics, details in Methods), this calibration measurement established a [porin]:[lipid surface area] ratio for the vesicles. Electrophysiology can be used to quantify the number of *functional* porins in the membrane which, as far as we know, is not possible with any other technique. However, the OmpF concentrations used for this calibration had to be much lower than the concentration used in the optofluidics assay, since higher porin concentrations prevented the formation of stable patches. Our results yielded an estimate of ~1800 porins per μm<sup>2</sup> for the proteoliposomes used in the optofluidics assay (Supplementary Figure S2). It is interesting to compare this result to the estimated number of general diffusion porins found in a typical bacterial cell; these porins are found in excess of 10<sup>5</sup> copies per cell<sup>6</sup>. This translates into an approximately 6–7× higher [porin]:[lipid surface area] ratio than used in our experiments. We noted significant variability in the OmpF insertion efficiency among different vesicle batches for the Port-a-Patch characterization. We believe this is also the underlying reason for the spread in the permeability coefficients obtained in the optofluidics experiments (Figure 1c,f).

Using the Port-a-Patch calibration, we can estimate the total number of functional porins in each proteoliposome detected in the optofluidics assay, and hence can estimate the norfloxacin flux per porin for each proteoliposome. An average over all the proteoliposomes detected gives a norfloxacin flux value per porin of  $10 \pm 8$  molecules/s ( $N = 420$ ) at pH 7 and  $15 \pm 10$  molecules/s ( $N = 268$ ) at pH 5 (errors are standard deviations). Full details of the calculation are provided in the

Supporting Information. The errors are a direct consequence of the above-mentioned variability in OmpF insertion, as seen in the Supporting Information Figure S2. If we include a correction (details in Supporting Information) to account for the contribution of flux across the pure lipids,<sup>25</sup> the change in the final result is negligible, as expected considering the time scales of the measurement and the relatively slower transport through pure DPhPC lipids.<sup>25</sup>

These flux per porin values are based on the assumption that the OmpF insertion efficiency remains the same even at the higher OmpF concentrations used in the optofluidics assay. In support of this assumption, we observed a linear increase in OmpF insertions with OmpF concentration in the calibration measurements at low OmpF concentrations (Supplementary Figure S2). However, we cannot rule out aggregation effects, which may reduce the insertion efficiency at high OmpF concentrations. This could result in fewer functional porins in the proteoliposome membranes in the optofluidics assay. This implies that we are possibly underestimating the flux per porin and thus our results present a lower bound for this value.

Our analysis of norfloxacin transport through porins and lipids has thus clarified some of the mechanisms by which drug transport is affected under changing external conditions. The optofluidics assay also presents a direct visualization of norfloxacin uptake across a proteoliposome membrane in a microfluidic, label-free system, not previously possible. The results unambiguously confirm the importance of these porins in facilitating the transport of fluoroquinolone antibiotics across the bacterial OM. In addition, our optofluidic technique enables the measurement of contributions to diffusion from pure lipids<sup>25</sup> and through porins, which cannot be done in a quantitative manner using the established liposome swelling assays.<sup>7,32,33</sup> Furthermore, our microfluidic based approach has the potential to explore a wide range of porins. Proteoliposomes could be devised containing a combination of passive diffusion porins and active transporters, to study competition between these processes. New vesicle preparation techniques<sup>34</sup> have shown considerable promise for integration into lab-on-a-chip devices and for the production of more homogeneous vesicle populations, which should translate into better control over porin insertions and proteoliposome modification. A combination of traditional and advanced single vesicle techniques can thus be used to investigate a variety of drug transport phenomena, an urgent need in medicine today.

## METHODS

**Optofluidic Permeability Assay.** The optofluidic permeability assay builds on our previous work studying the permeability coefficient of norfloxacin across lipid membranes.<sup>25</sup> It was designed to explore properties of porin mediated transport not accessible to electrophysiology and other traditional techniques. It enables the study of drug transport through porins without the application of a transmembrane voltage. Furthermore, even though electrophysiology has been the method of choice for characterizing antibiotic-porin interactions at the single molecule level,<sup>35–38</sup> it suffers from an inability to distinguish molecules that translocate through the porin from molecules that simply bind transiently.<sup>27</sup> The optofluidic permeability assay visualizes drug transport directly, by observing the drug molecules themselves via their autofluorescence; it is thus label-free. Liposome swelling assays<sup>32,33</sup> were previously used as an alternative to electrophysiology. However, these measure antibiotic flux relative to the flux of a permeable sugar (generally arabinose) and hence cannot measure drug permeability directly. Furthermore, the diffusion of charged compounds in these assays is influenced by the buildup of Donnan potentials inside the liposomes, which can lead to unexpected

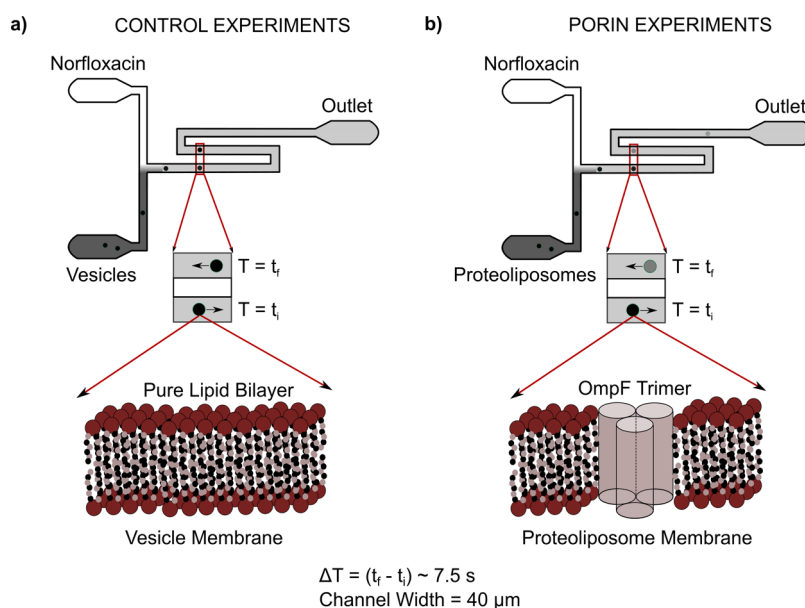


**Figure 3.** Schematic of the optofluidic permeability assay. Control experiments (no porin) are represented in (a) and proteoliposome experiments (containing OmpF) in (b). Vesicles (liposomes/proteoliposomes) are mixed with norfloxacin in a T junction microfluidic chip by applying suction at the outlet reservoir with a syringe pump; norfloxacin autofluorescence is stimulated with a UV epifluorescence microscope. The vesicles are detected at an initial time  $t_i$  immediately post mixing and at a later time  $t_f$ , a distance of 7.4 mm further downstream. Vesicles took, on average, about 7.5 s to travel the intervening distance. Both time points are observed in the same field of view. Detection of the autofluorescence intensities within the vesicles at both points enables the calculation of the drug permeability coefficient for each vesicle.

osmotic behavior.<sup>32</sup> Our assay overcomes many of these intrinsic limitations and provides a new technique for studies of drug transport with porins.

As described in Figure 3, the optofluidic permeability assay involves a T junction microfluidic chip where the vesicles (liposomes/proteoliposomes) and the drug molecules are mixed in a channel (via the application of suction at the outlet). The T junction geometry of the chip leads to an equal mixing of vesicle and drug solutions. The inlet norfloxacin concentration is 2 mM (prepared in the same buffer solution as the vesicles) and hence the vesicles are exposed to a final norfloxacin concentration of 1 mM. The vesicles are imaged immediately post mixing with the norfloxacin and at a distance 7.4 mm further along the channel; the chip was designed such that both points were observed in the same field of view (Figure 3). The chip design was based on preliminary experiments which showed that a distance of about 7–8 mm between the two points was optimal for the detection of proteoliposomes showing increased uptake of the drug.

The norfloxacin molecules were tracked by stimulating their autofluorescence in the UV.<sup>25</sup> We performed all the optofluidics experiments described in this paper on a commercial Olympus IX73 microscope, using a DAPI filter set (Chroma) and a Mercury arc lamp (Prior Lumen 200). A 60 $\times$  air objective was used (Olympus LUCPlanFLN, NA 0.70). Images were recorded using a scientific CMOS camera (optiMOS, QImaging) which enabled recording at 100 fps (10 ms exposure, bin 4). The microfluidic flows were controlled using a neMESYS syringe pump with a 250  $\mu\text{L}$  Duran Borosilicate glass syringe (ILS, Germany) connected to the outlet. At the beginning of the experiments, a flow of 30–40  $\mu\text{L}/\text{h}$  was applied until the autofluorescence intensity in the microfluidic channel reached its peak, ensuring an appropriate drug concentration in the channel. Once this level was reached, the flow was slowed to 3  $\mu\text{L}/\text{h}$  enabling the detection of individual vesicles for multiple frames as desired.<sup>25</sup>

The images were recorded using Micromanager 1.4<sup>39</sup> and analyzed in MATLAB (scripts available on request) to obtain information about the autofluorescence intensities within the vesicles, in addition to the background intensity, vesicle shape and velocity.<sup>25</sup> Upchurch 1520 G tubing (inner diameter 0.03 in.) was used to connect the outlet of the chip to the syringe. Full details of the mathematical model and permeability coefficient calculations can be found in the earlier

paper.<sup>25</sup> Calculations of the flux are presented in the [Supporting Information](#) document.

**Microfluidic Chip Fabrication.** The microfabrication of the fluidic chip relies on photolithography and replica molding. For the fabrication of the mold, a Silicon substrate was covered with a thin layer of adhesion promoter (Omnicore, Microchem, spin coating: 2000 r.p.m., 30 s). A layer of SU-8 2025 (Microchem) was then deposited (2000 r.p.m., 30 s), prebaked (2 min at 65  $^{\circ}\text{C}$ , 5 min at 95  $^{\circ}\text{C}$ ) and selectively exposed to ultraviolet light (12 s, 365–405 nm, 20  $\text{mW cm}^{-2}$ ) through a bespoke pellicle mask (Photodata Ltd., CAD file available on request). The sample was postbaked (1 min at 65  $^{\circ}\text{C}$ , 3 min at 95  $^{\circ}\text{C}$ ), developed for 3 min, dried with a gentle stream of Nitrogen and hard baked for 5 min at 95  $^{\circ}\text{C}$ .

Sylgard 184 polydimethylsiloxane (PDMS) was used to create a negative replica from the Silicon mold using standard soft lithography techniques<sup>40</sup> with an elastomer:curing agent ratio of 9:1 (Dow Corning). The PDMS mixture was poured onto the Silicon mold and baked at 60  $^{\circ}\text{C}$  for 55 min. The PDMS chip was then peeled off the mold and inlet/outlet columns created using a 1.5 mm biopsy punch (Miltex). The chip was plasma bonded to a glass coverslip (Type I, Assistant, Germany) using an air plasma (10 W, 25 sccm, 10 s exposure, Diener Electronic GmbH & Co. KG, Germany). Post plasma bonding, the chip was left in an oven at 60  $^{\circ}\text{C}$  for 5–10 min to enhance the adhesion of PDMS to glass.

**Vesicle Formation and OmpF Incubation.** Giant unilamellar vesicles (GUVs) of 1,2-diphytanoyl-*sn*-glycero-3-phosphocholine (DPhPC) lipids (Avanti Polar Lipids) were prepared via electroformation using a Nanion Vesicle Prep Pro (Nanion Technologies GmbH, Germany) setup as described previously.<sup>25</sup> The GUVs were prepared in 200 mM Sucrose with 5 mM Phosphate Buffer (pH 7) or 5 mM Acetic Acid (pH 5).

The OmpF incubation followed previously established protocols.<sup>41</sup> Purified stock OmpF (5.5 mg/mL) in a detergent, a 1% solution of *n*-octylpolyoxyethylene (octyl-POE, Bachem) prepared in Milipore water, was diluted 1:1 in the same detergent and vortexed; 1  $\mu\text{L}$  of this freshly diluted OmpF solution was added to 199  $\mu\text{L}$  of the vesicle stock solution and incubated at room temperature for an hour. Biobeads SM-2 (Bio-Rad) were added to remove the detergent and the mixture was incubated at room temperature for 45–60 min

followed by storage at 4 °C overnight. The next day, the OmpF embedded proteoliposome solution was separated from the Biobeads with a pipet and the sample used directly in experiments. For the control (liposome) experiments, 1  $\mu$ L of 1% octyl-POE (instead of the OmpF solution) was added to 199  $\mu$ L of the vesicles; the rest of the incubation protocol remained unchanged.

**Single OmpF Porin Ionic Current Measurements in a Solvent-Free Lipid Bilayer.** Reconstitution experiments and noise analyses were performed as described in detail previously.<sup>42</sup> The Montal and Mueller technique<sup>43</sup> was used to form a phospholipid bilayer using DPhPC (Avanti polar lipids). A Teflon film comprising an aperture of approximately 30–60  $\mu$ m in diameter was placed between the two chambers of a cuvette. The aperture was preprepared with 1% hexadecane in hexane for stable bilayer formation. 1 M KCl in 5 mM potassium acetate (pH 5) or 5 mM phosphate (pH 7) was used as the electrolyte solution and added to both sides of the chamber. Ionic currents were detected using standard silver–silver chloride electrodes from WPI (World Precision Instruments) that were inserted in both sides of the cuvette. Single channel measurements were performed by adding the protein to the *cis* side of the chamber (the side connected to the ground electrode). Spontaneous channel insertion was typically obtained while stirring the solution in the cuvette under an applied transmembrane voltage. After a successful single channel reconstitution, the *cis* side of the chamber was carefully perfused to remove any remaining porins, thus preventing further channel insertions. Conductance measurements were performed using an Axopatch 200B amplifier (Molecular Devices) in voltage clamp mode. Signals were filtered by an on-board low pass Bessel filter at 10 kHz with a sampling frequency of 50 kHz. Amplitude, probability and noise analyses were performed using OriginPro 8 (OriginLab) and Clampfit software (Molecular Devices). Single channel analysis was used to determine the antibiotic binding kinetics. In a single channel measurement, the quantities measured were the duration of blocked levels/residence times ( $\tau_c$ ) and the frequency of blockage events ( $\nu$ ). The association rate constant  $k_{on}$  was derived using the number of blockage events,  $k_{on} = \nu/3[c]$ , where  $[c]$  is the concentration of the antibiotic. The dissociation rate constant ( $k_{off}$ ) was determined by averaging the  $1/\tau_c$  values recorded over the entire concentration range.<sup>38</sup>

**Port-a-Patch Calibration for Estimating the OmpF Porin Concentration in Proteoliposomes.** The Port-a-Patch calibration measurement involves patching OmpF embedded proteoliposomes and counting the number of OmpF porins in a patch using electrophysiology. This measurement reveals the number of OmpF porins per unit area on the surface of the proteoliposomes.

Planar lipid bilayers were obtained from proteoliposomes prepared using the same protocols described earlier. Purified stock OmpF (5.5 mg/mL) porins in 1% octyl-POE were diluted in the detergent and reconstituted into GUVs by incubating the porins as described previously; however, the final porin concentrations used in the Port-a-Patch calibration experiments were a factor of 500 $\times$ , 250 $\times$  and 100 $\times$  more dilute than the final concentration used in the optofluidics assay to enable the counting of single porin insertions in the ionic current traces. After incubation, the detergent was removed using Biobeads SM-2 (Bio-Rad) as described previously. The Biobeads were discarded after centrifugation and the protein containing GUVs (proteoliposomes) used immediately.

For the formation of a planar lipid bilayer containing the proteins, 5  $\mu$ L of the proteoliposome solution was pipetted into 5  $\mu$ L of the electrolyte solution (200 mM KCl, 5 mM acetic acid for pH 5 or 5 mM phosphate for pH 7). The resulting solution was placed on a microstructured glass chip (grounded side) containing an aperture approximately 1  $\mu$ m in diameter. The vesicles burst once they touch the glass surface of the chip thus forming a planar lipid bilayer; additional suction was applied to patch proteoliposomes across the aperture. Ionic current measurements were performed using the same equipment and software as for the black lipid membrane measurements described above. The number of OmpF porins in a patch is calculated from the ionic current of the patch (Supplementary Figure S2), since the conductance of a single OmpF channel is known (the

conductance of the OmpF trimeric porin is  $0.9 \pm 0.1$  nS in 200 mM KCl at pH 7;  $N = 20$  individual porins were measured<sup>42</sup>). In the absence of OmpF porins, the ionic conductance of the patch is negligible, the bilayer makes a tight seal across the aperture. This difference in ionic current provides the basis for counting the number of porins in a patch.

## ■ ASSOCIATED CONTENT

### Supporting Information

The Supporting Information is available free of charge on the ACS Publications website at DOI: 10.1021/jacs.5b08960.

Additional experimental data for the optofluidic assay from two more distinct batches of proteoliposomes at each pH. Port-a-Patch calibration measurement for estimation of porin density in the proteoliposomes. Detailed explanation of the flux calculation. Explanation of data analysis in the optofluidic assay. Power spectrum of ion current in the presence of OmpF porins in the Port-a-Patch calibration. (PDF)

## ■ AUTHOR INFORMATION

### Corresponding Author

\*ufk20@cam.ac.uk

### Author Contributions

#JC and HB contributed equally to this work.

### Notes

The authors declare no competing financial interest.

## ■ ACKNOWLEDGMENTS

This work was supported by a European Research Council (ERC) Grant (261101 Passmembrane) to UFK. JC acknowledges support from an Internal Graduate Studentship, Trinity College, Cambridge, and a Research Studentship from the Cambridge Philosophical Society. SP was supported by the Leverhulme Trust through an Early Career Fellowship. TM acknowledges support from the Konrad-Adenauer Foundation and the German National Merit Foundation. HB, YB and MW are part of the TRANSLOCATION consortium and have received support from the Innovative Medicines Joint Undertaking under grant agreement 115525, the European Union's seventh framework program (FP7/2007-2013), and European Federation of Pharmaceutical Industries and Associates companies in-kind contribution. We thank Avelino Javier for help with the MATLAB scripts and Catalin Chimerele for helpful discussions.

## ■ REFERENCES

- (1) Allen, H. K.; Donato, J.; Wang, H. H.; Cloud-Hansen, K. A.; Davies, J.; Handelsman, J. *Nat. Rev. Microbiol.* **2010**, *8*, 251–259.
- (2) Cantas, L.; Shah, S. Q. A.; Cavaco, L. M.; Manaia, C. M.; Walsh, F.; Popowska, M.; Garelick, H.; Bürgmann, H.; Sörum, H. *Front. Microbiol.* **2013**, *4*, 1–14.
- (3) McKenna, M. *Nature* **2013**, *499*, 394–396.
- (4) Davies, J.; Davies, D. *Microbiol. and Mol. Biol. Rev.* **2010**, *74*, 417–433.
- (5) Ling, L. L.; Schneider, T.; Peoples, A. J.; Spoering, A. L.; Engels, I.; Conlon, B. P.; Mueller, A.; Schäberle, T. F.; Hughes, D. E.; Epstein, S.; Jones, M.; Lazarides, L.; Steadman, V. A.; Cohen, D. R.; Felix, C. R.; Fetterman, K. A.; Millett, W. P.; Nitti, A. G.; Zullo, A. M.; Chen, C.; Lewis, K. *Nature* **2015**, *517*, 455–459.
- (6) Delcour, A. H. *Biochim. Biophys. Acta, Proteins Proteomics* **2009**, *1794* (5), 808–816.
- (7) Pagès, J.-M.; James, C. E.; Winterhalter, M. *Nat. Rev. Microbiol.* **2008**, *6*, 893–903.



- (8) Redgrave, L. S.; Sutton, S. B.; Webber, M. A.; Piddock, L. J. V. *Trends Microbiol.* **2014**, *22* (8), 438–445.
- (9) Chevalier, J.; Malléa, M.; Pagès, J.-M. *Biochem. J.* **2000**, *348*, 223–227.
- (10) Hirai, K.; Aoyama, H.; Suzue, S.; Irikura, T.; Iyobe, S.; Mitsuhashi, S. *Antimicrob. Agents Chemother.* **1986**, *30*, 248–253.
- (11) Cohen, S. P.; McMurry, L. M.; Hooper, D. C.; Wolfson, J. S.; Levy, S. B. *Antimicrob. Agents Chemother.* **1989**, *33*, 1318–1325.
- (12) Kishii, R.; Takei, M. *J. Infect. Chemother.* **2009**, *15*, 361–366.
- (13) Stavenger, R. A.; Winterhalter, M. *Sci. Transl. Med.* **2014**, *6*, 228ed7.
- (14) Hooper, D. C. *Clin. Infect. Dis.* **2001**, *32* (Suppl. 1), S9–S15.
- (15) Zeiler, H. J. *Antimicrob. Agents Chemother.* **1985**, *28*, S24–S27.
- (16) Hooper, D. C.; Wolfson, J. S.; Souza, K. S.; Ng, E. Y.; McHugh, G. L.; Swartz, M. N. *Antimicrob. Agents Chemother.* **1989**, *33*, 283–290.
- (17) Smith, J. T.; Ratcliffe, N. T. *Infection* **1986**, *14* (Suppl.1), S31–35.
- (18) Nikaido, H.; Thanassi, D. G. *Antimicrob. Agents Chemother.* **1993**, *37*, 1393–1399.
- (19) Piddock, L. J. V.; Jin, Y.-F.; Ricci, V.; Asuquo, A. E. *J. Antimicrob. Chemother.* **1999**, *43*, 61–70.
- (20) Thomas, A. D.; Booth, I. R. *J. Gen. Microbiol.* **1992**, *138*, 1829–1835.
- (21) Sen, K.; Hellman, J.; Nikaido, H. *J. Biol. Chem.* **1988**, *263* (3), 1182–1187.
- (22) Kennedy, E. P. *Proc. Natl. Acad. Sci. U. S. A.* **1982**, *79*, 1092–1095.
- (23) Mortimer, P. G.; Piddock, L. J. *J. Antimicrob. Chemother.* **1991**, *38*, 639–653.
- (24) Kaščáková, S.; Maigre, L.; Chevalier, J.; Réfrégiers, M.; Pagès, J. M. *PLoS One* **2012**, *7*, e38624.
- (25) Cama, J.; Chimere, C.; Pagliara, S.; Javer, A.; Keyser, U. F. *Lab Chip* **2014**, *14*, 2303–2308.
- (26) Angelova, M. I.; Dimitrov, D. S. *Faraday Discuss. Chem. Soc.* **1986**, *81*, 303–311.
- (27) Mahendran, K. R.; Hajjar, E.; Mach, T.; Lovelle, M.; Kumar, A.; Sousa, I.; Spiga, E.; Weingart, H.; Gameiro, P.; Winterhalter, M.; Ceccarelli, M. *J. Phys. Chem. B* **2010**, *114*, S170–S179.
- (28) Benz, R.; Schmid, A.; Vos-Scheperkeuter, G. H. *J. Membr. Biol.* **1987**, *100* (1), 21–29.
- (29) Schwarz, G.; Danelon, C.; Winterhalter, M. *Biophys. J.* **2003**, *84*, 2990–2998.
- (30) Bezrukov, S. M.; Berezhkovskii, A. M.; Szabo, A. J. *Chem. Phys.* **2007**, *127*, 115101.
- (31) Wilks, J. C.; Slonczewski, J. L. *J. Bacteriol.* **2007**, *189*, 5601–5607.
- (32) Nikaido, H.; Rosenberg, E. Y. *J. Bacteriol.* **1983**, *153*, 241–252.
- (33) Yoshimura, F.; Nikaido, H. *Antimicrob. Agents Chemother.* **1985**, *27*, 84–92.
- (34) Karamdad, K.; Law, R. V.; Seddon, J. M.; Brooks, N. J.; Ces, O. *Lab Chip* **2015**, *15*, 557–562.
- (35) Delcour, A. H. *FEMS Microbiol. Lett.* **1997**, *151*, 115–123.
- (36) Delcour, A. H.; Martinac, B.; Adler, J.; Kung, C. *Biophys. J.* **1989**, *56*, 632–636.
- (37) Buechner, M.; Delcour, A. H.; Martinac, B.; Adler, J.; Kung, C. *Biochim. Biophys. Acta, Biomembr.* **1990**, *1024*, 111–121.
- (38) Nestorovich, E. M.; Danelon, C.; Winterhalter, M.; Bezrukov, S. M. *Proc. Natl. Acad. Sci. U. S. A.* **2002**, *99*, 9789–9794.
- (39) Stuurman, N.; Amdodaj, N.; Vale, R. *Microscopy Today* **2007**, *15*, 42–43.
- (40) Qin, D.; Xia, Y.; Whitesides, G. M. *Nat. Protoc.* **2010**, *5*, 491–502.
- (41) Kreir, M.; Farre, C.; Beckler, M.; George, M.; Fertig, N. *Lab Chip* **2008**, *8*, 587–595.
- (42) Singh, P. R.; Ceccarelli, M.; Lovelle, M.; Winterhalter, M.; Mahendran, K. R. *J. Phys. Chem. B* **2012**, *116*, 4433–4438.
- (43) Montal, M.; Mueller, P. *Proc. Natl. Acad. Sci. U. S. A.* **1972**, *69*, 3561–3566.